

Article

# Patient Data Analysis with the Quantum Clustering Method

Shradha Deshmukh <sup>1,\*</sup>, Bikash K. Behera <sup>2</sup>  and Preeti Mulay <sup>1</sup>

<sup>1</sup> Department of Computer Science and Information Technology, Symbiosis Institute of Technology, Symbiosis International (Deemed University), Pune 412115, India

<sup>2</sup> Bikash's Quantum (OPC) Pvt. Ltd., Balindi, Mohanpur 741246, India

\* Correspondence: shradha.deshmukh.phd2020@sitpune.edu.in

**Abstract:** Quantum computing is one of the most promising solutions for solving optimization problems in the healthcare world. Quantum computing development aims to light up the execution of a vast and complex set of algorithmic instructions. For its implementation, the machine learning models are continuously evolving. Hence, the new challenge is to improve the existing complex and critical machine learning training models. Therefore, the healthcare sector is shifting from a classical to a quantum domain to sustain patient-oriented attention to healthcare patrons. This paper presents a hybrid classical-quantum approach for training the unsupervised data models. In order to achieve good performance and optimization of the machine learning algorithms, a quantum k-means (QK-means) clustering problem was deployed on the IBM quantum simulators, i.e., the IBM QASM simulator. In the first place, the approach was theoretically studied and then implemented to analyze the experimental results. The approach was further tested using small synthetics and cardiovascular datasets on a qasm simulator to obtain the clustering solution. The future direction connecting the dots is the incremental k-means algorithm with the quantum platform, which would open hitherto unimaginable technological doors.

**Keywords:** quantum computing; machine learning; k-means clustering; quantum clustering; clustering algorithm; quantum k-means algorithm; quantum machine learning



**Citation:** Deshmukh, S.; Behera, B.K.; Mulay, P. Patient Data Analysis with the Quantum Clustering Method. *Quantum Rep.* **2023**, *5*, 138–155. <https://doi.org/10.3390/quantum5010010>

Academic Editor: Antonio Manzanali

Received: 29 September 2022

Revised: 2 February 2023

Accepted: 6 February 2023

Published: 13 February 2023



**Copyright:** © 2023 by the authors. Licensee MDPI, Basel, Switzerland. This article is an open access article distributed under the terms and conditions of the Creative Commons Attribution (CC BY) license (<https://creativecommons.org/licenses/by/4.0/>).

## 1. Introduction

The real fascination with quantum computing lies in its consistent and continuous computation ability. That is why the actual implementations of quantum computing technology are all in inaccessible areas wherein continuous monitoring and observation are necessary, such as navigation, seismology, the pharma industry and many more. Quantum information processing (QIP) is the turning point in computer science, mathematics, physics and engineering [1]. QIP is an inference of quantum mechanics to fulfill an information processing objective. Classical and quantum information can be used jointly to comprehend phenomena that are impractical for classical information processing, such as the exploration of an unstructured database with a quadratic speedup. It is associated with the most exemplary conceivable classical algorithms [2].

Machine learning is another concept wherein machines are trained to solve problems with learning algorithms where machines are pre-arranged with the capacity to discover some structure concealed within data. In unsupervised learning, for performing any typical task, firstly “natural” clusters present in the raw and unstructured data are discovered [3].

The process of grouping datapoints (input data) based on their similarities is called clustering, described as an unsupervised learning problem to generate training data using a specific set of inputs but without any label. In order to make a collection of unlabeled data more comprehensible and manipulable, clustering is the process of looking for comparable structural features. Clustering helps in the analysis of unstructured data at the surface level. The density of the datapoints, graphing and the shortest distance are some of the factors that affect the cluster formation. The centroid-based clustering method is used to study or

analyze unstructured data. It bases its operation on how closely the datapoints resemble the selected center value. The datasets are separated into a predetermined number of clusters (a set of datapoints or group), and a vector of values references each cluster. The input data variable shows no difference and joins the cluster compared to the vector value. The initial step is to define the number of clusters. The k-means algorithm is a centroid-based clustering technique used for surfacing and optimizing huge amounts of data. Using a variety of distance metrics, such as the Minkowski distance [4], Manhattan distance and Euclidian distance, the clustering methods iteratively calculate the separation between the clusters and the characteristic centroids (center of the cluster). The massive collection of healthcare data consented to be easily accessible. However, it was complex data; therefore, it required a lot of work to efficiently evaluate the data to produce significant judgments or assessments of the patient's health. Therefore, a prompt and fast technique is needed to aid health researchers in creating efficient healthcare policies, drug recommendation systems and persona-specific health profiles. The quantum clustering method is used to recognize the complex data patterns from the patient data [5]. The suitability of the quantum clustering method for complex healthcare data is discussed in Section 3. To fully utilize the healthcare data research, clinicians use the quantum domain [6]. The strategies and methods to overcome some of the healthcare challenges by leveraging the power of quantum and ML include:

- Connect health data from disparate sources
- Determine effective treatments by identifying hidden patterns
- Enable personalized care with precision
- Exploring real-world clinical data for risk stratification
- Create efficiencies in healthcare administration workflows (billing for health usage etc.)
- Predicting disease progression through quantum power and using casual inference to improve patient outcomes.

The future of today's cutting-edge technology is quantum machine learning (QML) [7]. QML is the fusion of quantum computing and artificial intelligence that will alter the future in the area dedicated to developing quantum algorithms for machine learning tasks. QML fills the gaps between the theoretical advances in quantum computing and the deployed machine learning science [8]. QML focuses on offering synthesis that describes the most relevant machine learning algorithm in the quantum framework, reducing the complexity of the discipline involved. QML is a highly new field with much more growth, but we can already start to predict how it will impact our future [9].

There are a few standard algorithmic primitives that are utilized to construct the algorithms in the majority of quantum machine learning applications. Quantum techniques for linear algebra, such as matrix multiplication and inversion, have been applied, for example, to recommendation systems. Second, supervised or unsupervised learning has used the capacity to estimate the separations between quantum states, for instance using the SWAP test [10]. Most of these processes require access to the data on a quantum level, which can be accomplished by storing the data in particular data structures [11].

Quantum interference is used to modify the underlying probabilities and helps with the quadratic speedup using Grover's search algorithm. Regarding the adiabatic optimization, the paper [12] explains many use case examples that talk about traffic optimization. Now, this is a slowly varying quantum evaluation. The paper [13] discussed solving energy minimization use cases. In the case of linear system algorithms, we leveraged Hamilton in the simulation to perform the matrix inversion. In the least-squares fitting, an exponential speedup for well-conditioned filling problems with sparse  $A$  is presented in [14]. The traditional math method requires hundreds of qubits [15]. We described QK-means algorithm, a quantum clustering algorithm that can be thought of as a quantum equivalent for the classical k-means algorithm. In more detail, the definition of the QK-means will be provided in Section 3. We present a comprehensive analysis to demonstrate that the QK-means produces results that are consistent with those of the classical k-means algorithm.

In this research paper, experimentation was performed using the quantum k-means (QK-means) clustering algorithm. Section 2 will cover the introduction and background research about the basics of quantum computing, machine learning, unsupervised clustering algorithm and the healthcare data-driven approach. Section 3 explains the methodology adopted for the quantum implementation of the QK-mean algorithm with the help of the state preparation process flow. The results and discussion portions are exhibited in Section 4, which presents the findings on two varieties of datasets.

### 1.1. Literature Review

The paper aims to improve the performance of clustering algorithms. The primary focus is to improve the QK-means algorithm's performance along with using fewer qubits. Beforehand, we studied the existing research by doing a literature review of the research papers in the field. The earlier works on clustering problems used the hybrid classical-quantum approach. In the paper "K-means clustering based on improved quantum particle swarm optimization algorithm", the authors used the k-means algorithm for faster convergence and accurate results [16]. The k-means algorithm was merged with an improvised version of the quantum particle swarm algorithm. The amalgamation of both algorithms provided an effective clustering result [16]. Another approach to using the k-means algorithm was implementing a quantum chaotic cuckoo search algorithm for data clustering [17]. The quantum chaotic cuckoo search algorithm combined the idea of a genetic cuckoo search, quantum algorithm and k-means algorithm. The performance of the hybrid k-mean algorithm was displayed in the form of the external and internal clustering quality. One would accept that it would have many enabled products in the healthcare space. However, the translation into the product has been relatively slow [18]. The different variants of the k-means algorithm used by researchers so far are shown in the following table (Table 1).

**Table 1.** Summary of existing variants of hybrid k-means quantum algorithm.

Sr. No.	Paper Title	Year of Publication	Authors	Methods
1	"A quantum-clustering optimization method for COVID-19 CT scan image segmentation" [19]	2021	Singh, P., Bose, S.S.	Proposed novel method for image segmentation grounded on k-means and fast forward quantum optimization
2	"Quantum spectral clustering" [20]	2021	Kerenidis, I., Landman, J.	Introduced quantum k-means algorithm for spectral clustering
3	"Quantum-inspired ant lion optimized hybrid k-means for cluster analysis and intrusion detection" [21]	2020	Chen, J., Qi, X., Chen, L., Chen, F., Cheng, G.	Merged quantum encouraged optimization with k-means algorithm for intrusion detection
4	"A Euclidean Group Assessment on Semi-Supervised Clustering for Healthcare Clinical Implications Based on Real-Life Data" [22]	2019	Sohail, M.N., Ren, J., & Uba Muhammad, M.	Improved the interpolative separable density fitting using the k-means algorithm and quantum approach
5	"Quantum algorithm for sequence clustering" [23]	2017	Bishwas, A.K., Mani, A., Palade, V.	Quantum paradigm for sequencing data using the hidden Markov model and k-means algorithm

### 1.2. Basic Concepts of Quantum Computing

This section explained a few core concepts of the quantum computing used. In quantum computing, the small unit of information is known as a qubit. Figure 1 depicts a glimpse of the basic principles of qubits and how they are pieces of the same concept. The binary notation and Dirac vector are used to represent the states (Equation (1)).

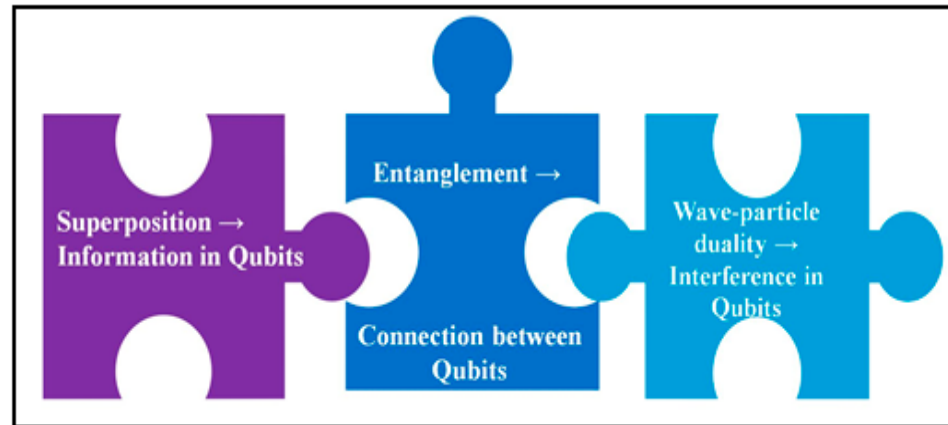


**Figure 1.** The figure shows the basic principles of qubits i.e., the superposition, entanglement and wave-particle duality. These principles contribute to achieving speedups in quantum computing.

$$|0\rangle = \begin{pmatrix} 1 \\ 0 \end{pmatrix} \text{ and } |1\rangle = \begin{pmatrix} 0 \\ 1 \end{pmatrix} \quad (1)$$

$$|\psi\rangle = (a|0\rangle + b|1\rangle) \quad (2)$$

where  $a$  and  $b$  are complex numbers and  $|a|^2 + |b|^2 = 1$ .

The 0 or 1 state is used to represent the classical algorithm, but in quantum computing  $|0\rangle$  and  $|1\rangle$  can be used at the same time with the handful probability of being in a state.

The state of a qubit is shown in Equation (2). The probability amplitude is for revealing one the states as an output where  $|a|^2$  and  $|b|^2$  are used for finding the probability of achieving  $|0\rangle$  and  $|1\rangle$ , respectively. The state of a qubit can also be written as  $|\psi\rangle = a|0\rangle + b|1\rangle$ . A qubit in such a state is said to be in superposition. So, once a measurement is completed on that qubit, it would yield  $|0\rangle$  with probability  $|a|^2$  and  $|1\rangle$  with probability  $|b|^2$ .

The quantum operations of the quantum gate are applied to transform and change the qubit states. The norm of the state vector is supposed to maintain the harmony after applying the quantum gate. It implies that the sum of the squares of the probability amplitudes should always be equal to one [24]. Hence, the unitary matrices are used to denote the quantum gates. It is a fact that all the quantum operations are reversible and do exist. All the quantum gates, except for the measurement gate, fall into this category. So, the non-reversible operation of the measurement gate is used at the end of the computation.

### 1.3. Model of Quantum Circuit

Quantum computation operates by harnessing a bundle of quantum gates on the qubits [25]. The quantum gates denote the quantum operations. As shown in Figure 2, there are three quantum gates directed to the qubits. The measurement is calculated at the end to obtain the outcome of the quantum circuit. This entire procedure of the quantum transition on the qubits is revealed in the system of a quantum circuit, where the timeline of the qubit is read from left to right. The quantum circuit model is the well-known method of evolving and exhibiting quantum models [26]. The three-qubit quantum circuit [27] that formulates entangled states is illustrated in Figure 2. The quantum circuit formulates this quantum state (Equation (3)). A quantum logic gate, often known as a “quantum gate,” is a

fundamental quantum circuit that uses a few qubits. To provide a clear image, Figure 2 depicts a quantum circuit example.

$$|\psi\rangle = \frac{1}{\sqrt{2}}|00\rangle + \frac{1}{\sqrt{2}}|11\rangle \quad (3)$$

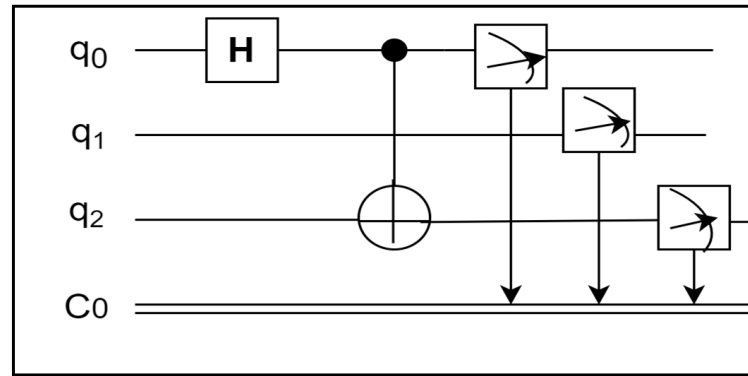


**Figure 2.** The quantum circuit for the three-qubit entanglement is depicted in the illustrations. Here, the controlled-NOT gate is applied, the Hadamard gate is applied to the qubits and the measurement is applied to every qubit.  $q_0$ ,  $q_1$  and  $q_2$  are the quantum registers and  $c_0$  classical register.

Figure 2 shows a quantum circuit for a two-qubit entanglement. On the qubit  $q_0$ , the Hadamard gate and the controlled-NOT gate are applied. The control and the target qubit are  $q_0$  and  $q_1$ , respectively. A measurement gate is applied to both the  $q_0$  and  $q_1$  qubit at the termination of the circuits.

## 2. The QK-Means Algorithm

We are focused on unsupervised learning and, more specifically, the classic clustering problem. Given a dataset represented as  $N$  datapoints (vectors), we assigned the vectors to one of the  $k$  labels. The initial stage defined the number of  $C$  or used an elbow method to identify the best value of  $C$  so that similar datapoints are assigned to the same cluster. The Euclidean distance is frequently used to evaluate how similar datapoints are grouped. However, different metrics may be appropriate depending on the problem. To understand the QK-means algorithm, it was important to know the basics about the working of the  $k$ -means algorithm (Table 2). The  $k$ -means clustering was composed of four essential stages as explained in Table 3. The QK-means firstly identified the preliminary value of the centroids (center of the cluster). Let  $(C_1, C_2, \dots, C_{n-1}, C_n)$  represent the centroid's harmony. The Euclidean distance was used to calculate distances and then the distance matrix at iteration 0 was executed. The flow of encoding, distance calculation and centroid assignment are shown in Figure 3. A matrix  $V \in R^{N \times d}$  was used to describe the dataset; each row is a vector  $V_i \in R^d$  for  $V \in [N]$  that represents one datapoint. The centroid of the cluster  $C_i$  for the  $j^{\text{th}}$  row is  $j \in [k]$ . We employed a tool created in [8] in addition to the amplitude to increase the likelihood of achieving an accurate estimate for the distances needed for the QK-means algorithm. In order to calculate the median, we took several copies of the estimator from the amplitude estimation technique. A series of quantum algorithms was created for the encoding of the classical data into quantum data by the quantum computing approach known as amplitude amplification [28,29], which generalizes the concept behind Grover's search algorithm. We assumed that the state space of our quantum system was represented by an  $N$ -dimensional Hilbert space (Equation (4)). If the dataset has  $V$  points

overall, we could locate them by initializing a quantum register  $|\psi\rangle$  with  $n$  qubits where  $2^n = N$  into a uniform superposition of each dataset and datapoint  $N$  such that:

$$|\psi\rangle = \frac{1}{\sqrt{N}} \sum_{k=0}^{N-1} |k\rangle \tag{4}$$

**Table 2.** Basic steps for the classical k-means algorithm [30,31].

Step 1:	Define the number of clusters
Step 2:	Randomly pick the centroid
Step 3:	Calculate the distance between the datapoints and centroids
Step 4:	Assortment based on the minimum distance
Step 5:	All the datapoints converges or no movement
Step 6:	Stop the iterations

**Table 3.** The steps shows the general stages of the quantum k-means algorithm [15,32,33].

Quantum K-Means General Steps	
	Initialization
<b>Step 1:</b>	$ Y\rangle = \{ y_n\rangle \in C^j, j = 1, 2, 3, \dots, N\}, K,$ The centroid (center) of the cluster is $X$ . Where $X =  x_1\rangle,  x_2\rangle, \dots,  x_k\rangle$
	Cluster Assignment
<b>Step 2:</b>	Each datapoint assigned to the nearest cluster $C_{k^*} \rightarrow \{ y_n\rangle : d_q^2( y_n\rangle,  x_{k^*}\rangle) \leq d_q^2( y_n\rangle,  x_k\rangle),$ $\forall k, 1 \leq k \leq K\}$
	Centroid updation
<b>Step 3:</b>	$K = \{1, 2, 3, \dots, K\},$ Updation of the centroid for each cluster $ x_k\rangle \rightarrow  G_K^T Y\rangle$
<b>Step 4:</b>	Redo the steps until all the datapoints converged

The QK-means algorithm at a high level accomplishes in the identical method as the classical k-means algorithm. Therein, the quantum subroutines are used for the distance estimation, then the least value out of the set of elements is discovered. Subsequently, the matrix multiplication for the procurement of the new centroids as quantum states and effectual tomography is achieved. Some random initial points should be picked, primarily when using, for example, the k-means [26]. Assigning the clusters is achieved by executing Steps 1 and 2. Step 3 and Step 4 calculate the minimum distance and assign a datapoint to the nearest centroid. In this way, the whole process is restated until the convergence is achieved (Figure 3). By using encoding techniques, all the classical data are transformed into a quantum state. For additional processing, the amplitude encoding technique is utilized. The QK-means algorithm is used to evaluate all the performance metrics as those of the classical algorithm to perform the comparative analysis after data preprocessing (normalization and outlier rejection). The accepted input data form is quantitative data i.e., numeric data. Refs. [34,35] brought up the issue with the dead units. In other words, if certain units are initialized more distantly from the input dataset than other units, they instantly stop learning throughout the whole learning process. Due to the fact that only the Euclidean distance is used for clustering, it suggests that the data clusters are formed similar to balls. The cluster number must be predetermined. The k-means algorithm can accurately identify the clustering centers when  $k = k^*$ . Otherwise, some datapoints will not be positioned at the centers of the appropriate clusters, which would result in an inaccurate clustering result. Instead, they are either at locations where distinct clusters converge, or they are biased away from the specific cluster centers.

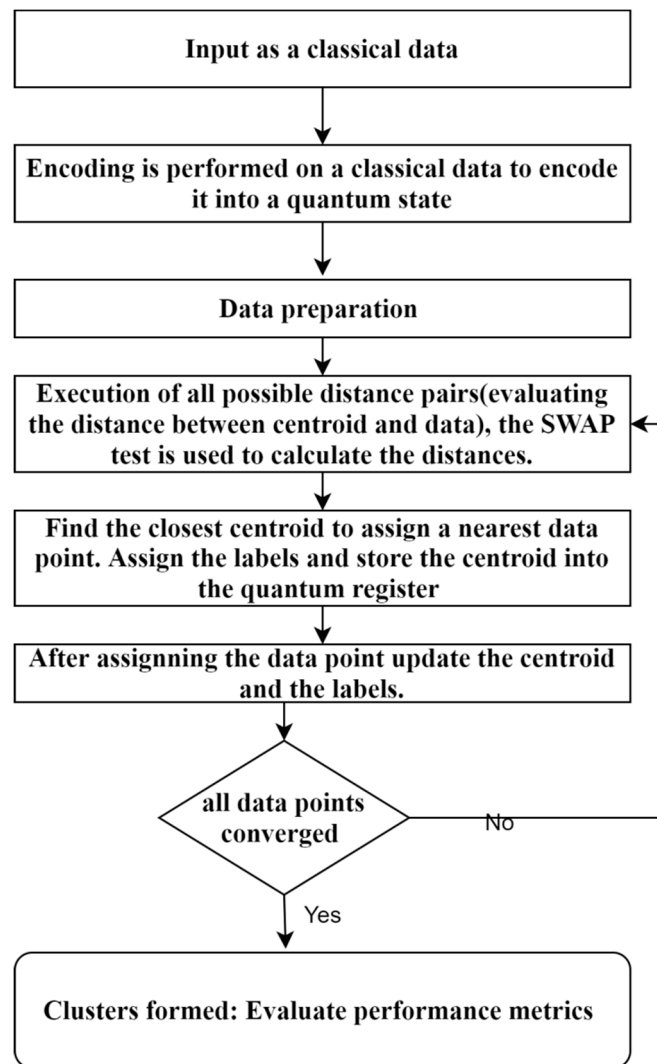


**Figure 3.** The process flow of the QK-means algorithm. The centroid is the cluster center and datapoints are the input vectors.

#### Step 1: Centroid Distance Calculation

The algorithm resumes with the estimation of the square distance between the data points and clusters with the help of a quantum procedure. To determine the square distance or inner product (with sign) between the two vectors contained in the QRAM, a quantum subroutine can be modified. When we achieved quantum access to the vectors and centroids, the distance estimation became very effective. We estimated the distances or inner products between the vectors with various standards in order to calculate the QK-means. On a high level, we then estimated the inner product of the unnormalized vectors by first estimating the inner products between the quantum states  $|V_i\rangle$  and  $|C_j\rangle$ , corresponding to the normalized vectors (Equation (5)), and then multiplying our estimator by the product of the vector norms. Instead of using the inner product, a comparable computation was conducted for the square distance. The square distance was calculated using the SWAP test as explained in [24] or using the distance calculation procedure as given in [36].

The probability of getting zero for each of the  $V_i$  is calculated using Equation (5).

$$\langle V_i | C_i \rangle = \sqrt{2P_0 - 1} \quad (5)$$

For calculating the distances for each and every datapoint, Equations (6) and (7) show the datapoints assigned to either cluster 1 or cluster 2, i.e.,  $C_1$  and  $C_2$ , respectively.

$$\langle V_1|C_1 \rangle, \langle V_2|C_1 \rangle, \langle V_3|C_1 \rangle, \dots, \langle V_n|C_1 \rangle \tag{6}$$

$$\langle V_1|C_2 \rangle, \langle V_2|C_2 \rangle, \langle V_3|C_2 \rangle, \dots, \langle V_n|C_2 \rangle \tag{7}$$

The  $U_3$  gate contains the encoding for the centroids and datapoints features. The first qubit receives the H gate, which connects the measurement to the conventional register. The entangled qubits carry out the SWAP test to determine the distance between the datapoints and centroids. The SWAP test is performed using a combination of control and anti-control gates. The distance between the first datapoint and centroid 1 ( $C_1$ ) is determined, as shown in Figure 4, and the distance between the first datapoint and centroid 2 ( $C_2$ ) is calculated. The probabilities of getting the nearest centroids are measured using the Z gate. The shots should be chosen according to the requirements and run on the IBM simulator after the circuit has been run. Place the  $P_0$  value into the calculation above  $\sqrt{(2P_0-1)}$  (Equation (5)) after calculating the frequency of achieving 0 and dividing it by the total number of shots.

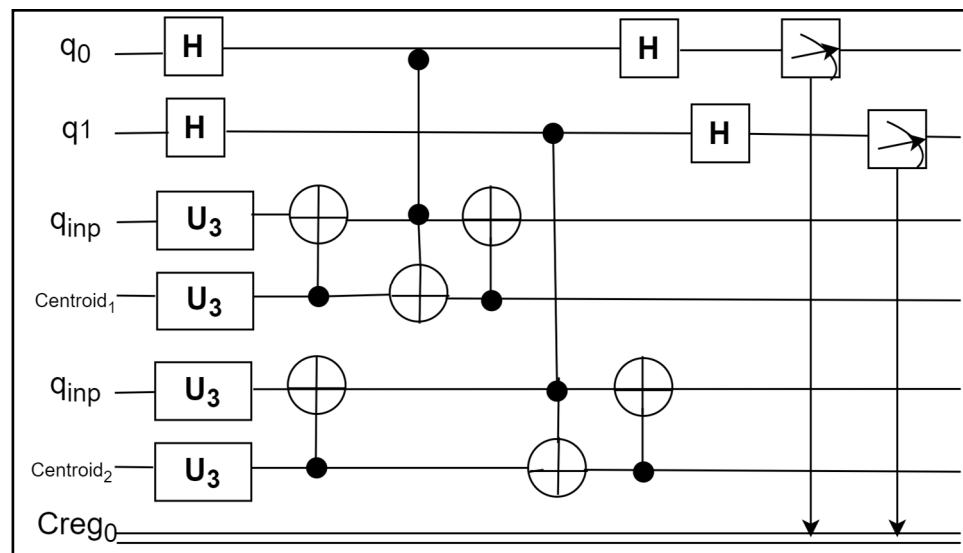


**Figure 4.** Using the Hadamard gate on the first qubit, the creation of the centroid distance estimate calculated the distance between the centroid and the datapoints using the SWAP test, then we performed the measurement to obtain the output.  $q_0$  and  $q_1$  are the quantum registers in superposition.  $q_{inp}$  is the quantum register which is used to encode the classical input datapoints. Centroid<sub>1</sub> and Centroid<sub>2</sub> quantum register encode the centroid value (cluster center),  $C_{reg_0}$  is the classical register.

**Step 2: Cluster assignment**

After the termination of Step 1, distinctly assess the distance between the datapoints and  $k$  centroid in the different registers and subsequently opt for the index  $j$  corresponding to the centroid adjoined to the given datapoint.

Now, initially take two points as the centroid (i.e.,  $C_1$  and  $C_2$ ). Calculate the distance from one datapoint to  $C_1$  and  $C_2$ , then obtain the closest centroid either  $C_1$  or  $C_2$  (Figure 5). Update one of the centroids for further calculation. Calculate the distances for all the data points until the final result appears as a new centroid or updated centroid. With the help of the new centroid, different clusters will be formed. To prepare the quantum state of the centroid, we need to make  $|C_1\rangle$  a tensor with all the datapoints in superposition.

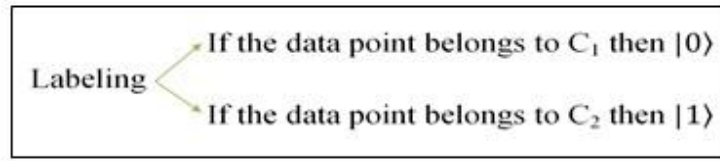


**Figure 5.** Labeling shows that the C1 cluster belong to the  $|0\rangle$  state and C2 cluster belongs to the  $|1\rangle$  state.

**Step 3: Centroid state creation**

The assignments of the centroid initially store the index of the datapoint and then store the label of the centroids. After updating the centroid in the iteration, the label values will be assigned to the datapoints.

The input data  $\sum |i_1\rangle$  is in superposition when

$$|\psi_{in}\rangle = |i_1\rangle|+\rangle + |i_2\rangle|+\rangle + |i_3\rangle|+\rangle + \dots + |i_n\rangle|+\rangle + \dots + \tag{8}$$

$$|\psi_{fin}\rangle = (|i_1\rangle|C_1\rangle \text{ or } |i_1\rangle|C_2\rangle) + (|i_2\rangle|C_1\rangle \text{ or } |i_2\rangle|C_2\rangle) + (|i_3\rangle|C_1\rangle \text{ or } |i_3\rangle|C_2\rangle) + \dots + (|i_n\rangle|C_1\rangle \text{ or } |i_n\rangle|C_2\rangle) + \dots + \tag{9}$$

While estimating the distance between the centroids and datapoints, the datapoints were assigned to their respective centroids. For assigning the clusters, we used a combination of quantum gates, i.e., the Hadamard gate, NOT gate, controlled-NOT gate and measurement. Initially, the input data  $\sum |i_1|+\rangle$  in the superposition implies that the datapoints are not assigned yet. Each time the centroid is updated in order to check which datapoints belong to which state, we needed to measure their corresponding qubits. Suppose that the qubits are in the  $|0\rangle$  or  $|1\rangle$  state. If they are  $|0\rangle$ , then the datapoint belongs to cluster 1 (C1) and if they are  $|1\rangle$ , then that datapoint belongs to C2 (Figure 6 and Equations (8) and (9)).

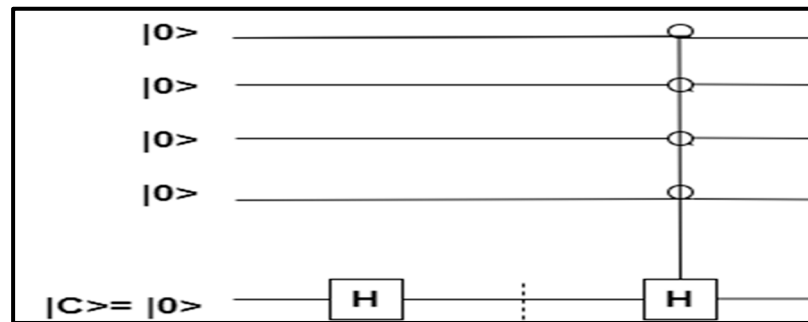


**Figure 6.** The pictorial description shows all the qubits in the  $|0\rangle$  state, which will apply when the datapoint belongs to label 1 or centroid 1.

**Step 4: Cluster Updation**

Check the first datapoint while taking into account the initial data. Then, take into account the separation between  $\langle i_1|K_1\rangle$  and  $\langle i_1|K_2\rangle$  (Figure 6). A SWAP test between  $i_1$  and  $K_1$  or  $K_2$  is conducted to determine which one will be at the shortest distance. A second qubit is used to hold the centroids. A new centroid value is encoded in the U gate for the cluster assignment. The centroid vectors are the input for rotating the value into the block sphere for a new centroid in the U gate. Take two qubits for  $|K_1\rangle$  and  $|K_2\rangle$  where continuous updating is required. After choosing the points for  $|K_1\rangle$  and  $|K_2\rangle$ , store those points in the qubits. As  $|K_1\rangle$  and  $|K_2\rangle$  can be prepared as taking the initial state  $|0\rangle$  and putting a U gate, similarly prepare  $|K_2\rangle$ . As a result of Step4 (Figure 7), each time  $|K_1\rangle$  and  $|K_2\rangle$  are updated, find the distances of the datapoints from the new  $|K_1\rangle$  and  $|K_2\rangle$  and

follow the same steps to calculate the distances. Show the datapoints in a single qubit system once the labeling of the datapoints is achieved. While doing the SWAP test, the circuit will deal with the data. However, the  $|\psi_{in}\rangle$  value (Equation (8)) will need labeling. For example, 16 datapoints need four qubits. Figure 7 shows the labeling of the datapoints. Implementing the quantum state for the labeling converted the  $|+\rangle$  state into the  $|0\rangle$  state. So, for that, we applied an H operation. If the result (probability) shows the  $|0\rangle$  state, then the answer is  $K_1$  and we conduct the following operation (Figure 6).

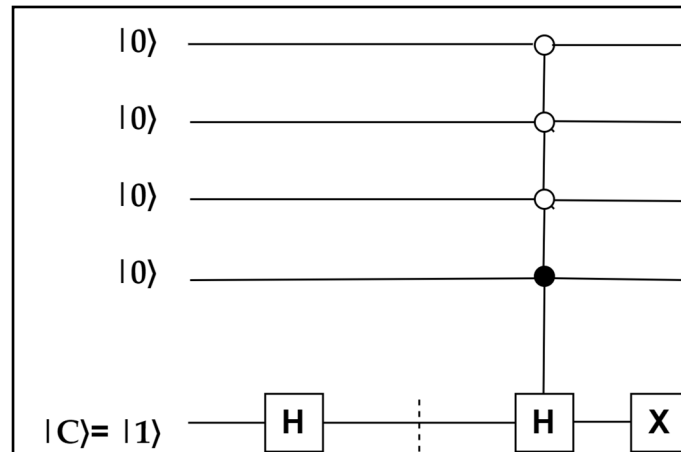


**Figure 7.** When a datapoint belongs to label 2 or centroid 2, as shown in the visual representation, all the qubits are in the  $|1\rangle$  state.

After updating  $|K_1\rangle$  and  $|K_2\rangle$ , again store them into the quantum state and then perform the SWAP test for second datapoint  $|i_2\rangle$  using a new centroid. If that second datapoint is nearest to  $|K_2\rangle$ , it belongs to C2 (i.e.,  $|1\rangle$ ). As shown in Figure 6, when the H gate is applied, the state becomes the  $|0\rangle$  state, and after applying the H gate and X gate consecutively, the final output is the  $|1\rangle$  state (Figure 7). At the end, apply the measurement to see which state the datapoints are in. The cluster assignment, which is a visual depiction of the label assignment, is shown in Figure 8.

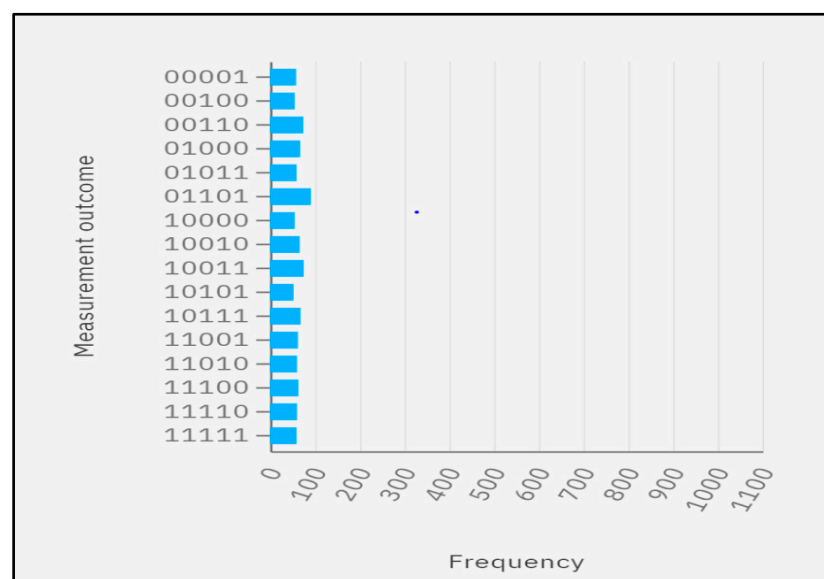


**Figure 8.** Result 1: Run on simulator which shows the measurement outcomes (probability).

To apply label 1 or centroid 1, a  $|0\rangle$  state is formed. To apply label 2 or centroid 2, a  $|1\rangle$  state is created. Table 4 shows that the centroids  $K_1$  and  $K_2$  belong to clusters  $C_1$  and  $C_2$ , respectively.

**Table 4.** Example, datapoint 1 (If 1 belongs to  $K_1$  it means it is in  $|0\rangle$  state).

$\langle K_1 \rangle$	$K_1 \in C_1$
$\langle K_2 \rangle$	$K_2 \in C_2$

### 3. Results and Observations

This section demonstrates the performance of the QK-means algorithm with two different datasets, i.e., the Mucormycosis and cardiovascular datasets (Table 5). The experiment shows the unsupervised learning to get the  $C$  number of clusters ( $C = 2$  or  $C = 3$ ). The clusters are then evaluated by the similarity measures to show the cluster quality and clustering with the defined clusters. We first discuss the clustering results from the small mucormycosis dataset (synthetic dataset) and then discuss the cardiovascular dataset. The accuracy rate ( $A$ ) (Equation (10)) shows the comparison between the different classical and classical-quantum algorithms.

$$A = \sum_{k=1}^n \frac{n(X_k)}{n} \quad (10)$$

where  $n(X_k)$  is the number of the quality cluster  $k$  and  $n$  is the total number of datapoints. The good clustering performance has the higher accuracy rate.

**Table 5.** Details of the datasets which contain characteristics of each datapoint, the number of clusters, the total number of datapoints and selected features.

Datasets	Characteristics	Clusters	Data Points	Features
Mucormycosis	Integer	2	16	2
Cardiovascular	Integer	2	6000	5

We measured all the data, which were calculated by observing the probabilities in order to obtain the clusters. We employed quantum circuits to store the clusters in the quantum data state and we also used the SWAP test to measure the Euclidean distance. The quantum component evaluated these two stages. The centroid (cluster centre) value was first defined (i.e.,  $k = 2$ ), and these two centroids were then labelled as label 0 and label 1. When the input data were labelled with the combination of anti-control and NOT operations, it was categorized as cluster 1 (label 1) and cluster 0 (label 0). It was crucial to first set up a circuit for the final output (Table 6), and only then were all the qubits measured. All of the states resulted from the H operation with equal likelihood. Using these steps, we gained the following two advantages:

- Calculating the distance between the two datapoints and storing huge amounts of data in the small amount of a qubit.
- Reduced research complexity.

We assigned the labelling of the centroid to the states with four qubits during the cluster assignment stage. As a result, the circuit's centroid labelling was used to assign the clusters. The circuit was created using the control NOT instead of the operation. The necessary qubit was the sum of all the classical registers. The measurement result was 00001, which denoted a cluster assignment of 0 (read from left to right) and a datapoint of 0001 (read from right to left) (Table 6). The synthetic input dataset contained the most datapoints and belonged to label 2. ( $C_2$ ). These datapoints were therefore given label 2 first, followed by label 1 for the remaining datapoints. Based on the likelihood determined by the QASM simulator (Figure 8). The measurement's probability demonstrated that the cluster assignment was done correctly (Figure 5). By computing the distance between

the clusters and the datapoints, the datapoints were assigned to the matching cluster. According to the results fetched from the QASM simulator, the datapoints  $|0000\rangle$ ,  $|0011\rangle$ ,  $|0100\rangle$ ,  $|0101\rangle$ ,  $|0111\rangle$ ,  $|1001\rangle$ ,  $|1010\rangle$  and  $|1100\rangle$  belonged to cluster 2 (C<sub>2</sub>) and the datapoints  $|0001\rangle$ ,  $|0010\rangle$ ,  $|0110\rangle$ ,  $|1000\rangle$ ,  $|1011\rangle$  and  $|1101\rangle$  belonged to cluster 1 (C<sub>1</sub>).

**Table 6.** Data points along with the labeling and cluster numbers (Mucormycosis dataset).

Data Points	Labeling	Cluster Assigned
0	0000	C <sub>2</sub>
1	0001	C <sub>1</sub>
2	0010	C <sub>1</sub>
3	0011	C <sub>2</sub>
4	0100	C <sub>2</sub>
5	0101	C <sub>2</sub>
6	0110	C <sub>1</sub>
7	0111	C <sub>2</sub>
8	1000	C <sub>1</sub>
9	1001	C <sub>2</sub>
10	1010	C <sub>2</sub>
11	1011	C <sub>1</sub>
12	1100	C <sub>2</sub>
13	1101	C <sub>1</sub>

Final Output =  $|0000\rangle|1\rangle + |0001\rangle|0\rangle + |0010\rangle|0\rangle + |0011\rangle|1\rangle + |0100\rangle|1\rangle + |0101\rangle|1\rangle + |0110\rangle|0\rangle + |0111\rangle|1\rangle + |1000\rangle|0\rangle + |1001\rangle|1\rangle + |1010\rangle|1\rangle + |1011\rangle|0\rangle + |1100\rangle|1\rangle + |1101\rangle|0\rangle$ .

- IBM QASM simulator
- Provider: imp-q/open/main
- 32 qubit simulator
- Simulator type: General, Context-Aware
- Version: 0.1.547
- Shots: 1024 and 8215

### 3.1. Results on Mucormycosis Dataset

The paper showed the implementation of a quantum clustering algorithm, i.e., the QK-means algorithm on a small dataset (a Mucormycosis dataset containing 16 datapoints), and the performance was compared with the classical k-mean algorithm (Figure 9). The size of the feature space affected the QK-means algorithm's completion time. It was presented through an examination of the QK-means algorithm, which depended on the characteristics of the data matrix.

The final result also implied that the improvised version of the QK-means performed much better than the k-means algorithm overall. Depending on the circuits and noise model, different simulation methods were available. The state console computer was described by a vector with  $2^n$  elements, what we call the statevector. The state vector simulator supported the additional configurable options and the advanced simulation methods. The instructions and gates were applied to simulate the quantum circuits by using the wave function of a statevector and also had the potential to support the general noise modeling. IBM provided the high performance QASM simulator for simulating the quantum circuits with and without noise.

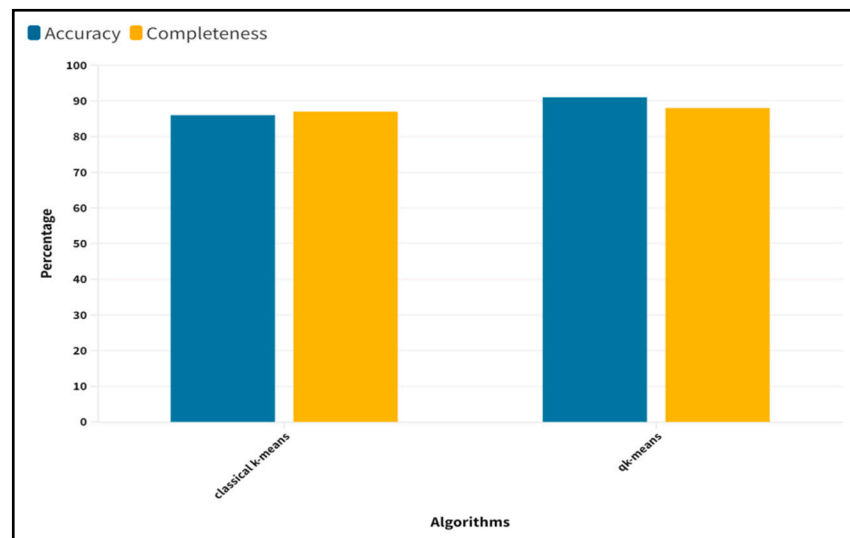


**Figure 9.** The bar graph shows the result of classical k-means algorithm and QK-means algorithm using the accuracy and completeness metrics on the Mucomycosis dataset.

### 3.2. Cardiovascular Dataset

A dataset from Kaggle.com was chosen in order to predict whether a person has cardiovascular disease [37]. This dataset included three different categories of data: factual information, examination feature results and patient-provided information. Additionally, the category and numerical data was separated from the dataset's data. The original dataset comprised 14 characteristics and 70,000 data instances. To compare the association between the age groups and cardiovascular disease, a graphical depiction was created (Figure 10). The graphic displays a bar chart with the number of persons on the Y-axis and their age in years on the X-axis. Figure 10 represents those with cardiovascular illness with the color purple, while those without the disease are shown in blue. People in the age range of 56 to 60 were definitely more susceptible to the condition, as shown by the graph. Additionally, as shown in Figure 11, a visual analysis of the categorical data distribution was carried out. The bivariate study discussed above demonstrated that the individuals with cardiovascular disease had higher blood sugar and cholesterol levels than non-sufferers. By eliminating the outliers, irrelevant data were omitted and the dataset was made more representative. Diastolic blood pressure ( $ap\_lo$ ) cannot be greater than systolic blood pressure ( $ap\_hi$ ) since the former refers to the pressure in the arteries between heartbeats, while the latter measures the greatest pressure the heart can exert while pumping. Additionally, blood pressure is the numerical difference between systolic and diastolic blood pressure; it cannot be minus. By taking into account these details, the anomalies from  $ap\_hi$  and  $ap\_lo$  were eliminated in order to remove erroneous blood pressure data. We observed an updated dataset with a new decreased number, which was equivalent to 6000 quantities of the dataset after the data cleansing process. We employed the amplitude encoding approach and the U3 gate to encode the features of the datapoints after cleaning the classical data with the help of classical preprocessing techniques to focus on the significant patient characteristics. Age, cholesterol, smoking, alcohol consumption and physical activity were the cardiovascular data characteristics we focused on. The amplitudes or features were arranged in a block sphere, and the quantum state was subjected to quantum processes to produce the clusters. The QK-means algorithm performed well on the data related to cardiovascular disease. Figure 12 presents the accuracy metrics for the QK-means algorithm's performance. Recent literature [38] provides a more detailed description of the measures used. The classical counterpart of the QK-means algorithm obtained an 82% accuracy, but the classical-quantum QK-means method achieved a 91% accuracy in clustering the input cardiovascular disease data, according to a comparison of the classical

k-means, k-means ++ and the QK-means algorithms. Finally, we showed that the QK-means converged more accurately than the classical clustering techniques (Figure 12). It was made possible due to the fluctuations that occurred more quickly from the fleeting equilibrium of the clusters.

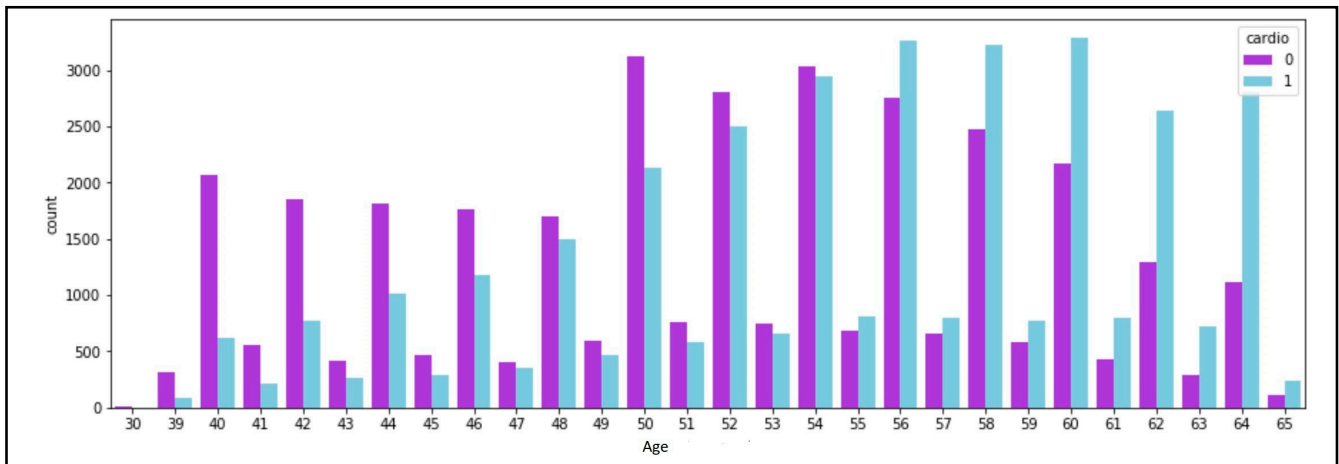


**Figure 10.** The graph above demonstrates that adults between the ages of 56 and 60 seem to be more susceptible to cardiovascular disease.

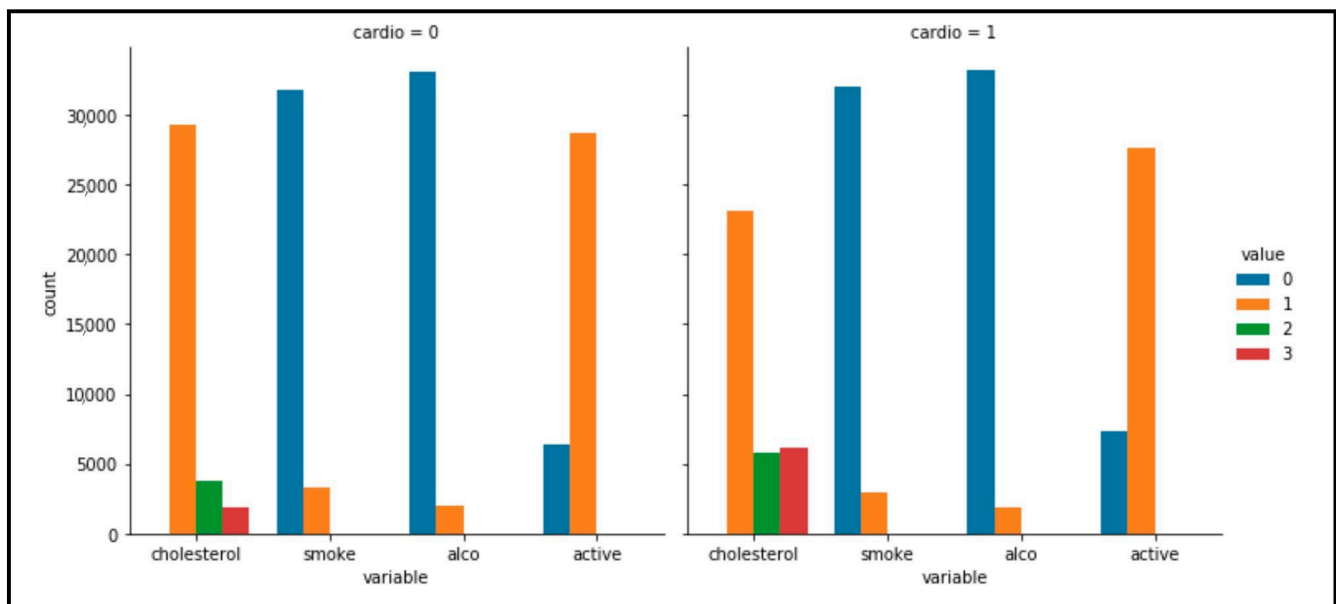


**Figure 11.** The cardiovascular dataset contains categorical variables such as glucose levels, cholesterol, smoking, drinking and physical activity. It is evident that those suffering from cardiovascular disease have higher blood sugar and cholesterol levels.

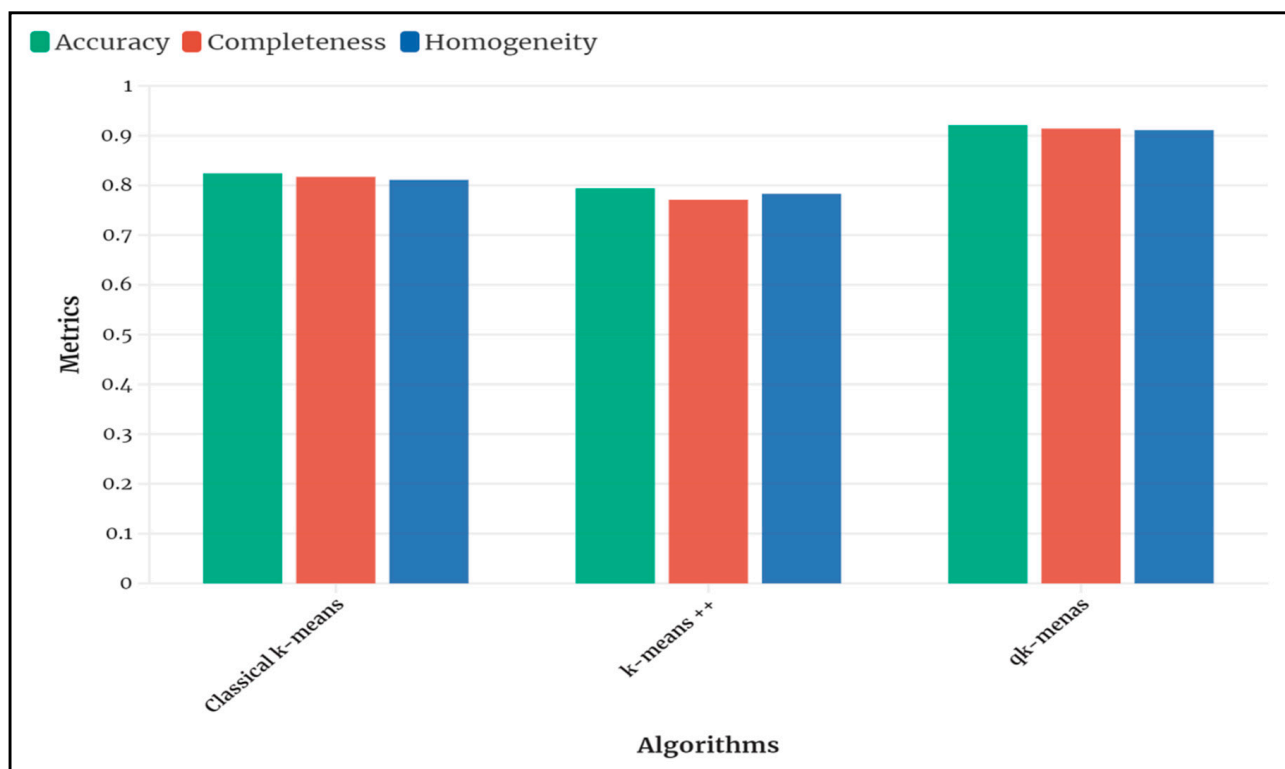


**Figure 12.** Results from the various classical and classical-quantum clustering algorithms, including the k-means, k-means++ and QK-means algorithms, are displayed in the bar graph using the cardiovascular dataset. Three metrics—accuracy, completeness and homogeneity—are employed.

#### 4. Conclusions and Future Direction

Quantum computing and its algorithms are being extensively used and effective in various applications. Looking at the track records of the quantum computers that provide exponential speedups and reduced work time, they are one of the first preferences of researchers all over the world. This added advantage of speedups proves to be a game changer for machine learning algorithms since training a data model is usually a time consuming process, as it involves a big deal of manipulation for the vectors. Hence, with newly emerging applications for machine learning models, a great deal of interest to improve the existing training algorithms has been noticed.

This study described a quantum adaptation of the classical k-means algorithm. In addition, we discussed how scaling would be possible in relation to the present iterations of the k-means and k-means++ clustering algorithms. Initially, it was discovered that complex datasets and tensor products may be deployed and computed quickly on quantum computers. However, there are other restrictions that also applied to this situation regarding noise and qubit coherence durations. These restrictions were also the reason for the ineffectiveness and decreased precision of problem-solving. In this research, we demonstrated the quantum implementation of the k-means algorithm on the IBM quantum QASM simulator using the SWAP test. To significantly improve the k-means technique, we constructed quantum clustering through employing intricate quantum circuits and a variety of quantum operations. The result in Section 4 demonstrated that the classical-quantum clustering QK-means algorithm outperformed the existing classical k-means and k-means++ algorithms in terms of cluster quality and accuracy.

The QK-means algorithm's limitation was that it must repeat each step when a new data series was added. After gathering the necessary data from the current clustering and existing dataset, the incremental clustering was applied to the incremental data. Without constantly scanning the dataset and executing the algorithm, the new data was matched in the already-existing clusters or formed in a new cluster. To overcome the classical problem in the QK-means, the quantum incremental k-means algorithm can be used. The steps of the proposed quantum incremental k-means algorithm are as follows.

Step 1: Estimate the centroid distance with the help of superposition.

Step 2: Perform entanglement to calculate closest distance between the datapoints and the centroids.

Step 3: For the centroid state, measure the label register and carry out the matrix multiplication.

Step 4: Using quantum tomography, update the calculated centroid.

Step 5: Repeat the steps until the formation of all clusters is achieved.

Steps 6: As new data arrives, use quantum parallelism for the best match.

In this study, we discussed the possibility of using quantum clustering techniques for two types of healthcare data which included a lower number of features. In the future, we will work on the complex feature-rich dataset (i.e., a large number of features). The quantum incremental k-means algorithm offered a different approach to learning from the data and aids in finding the needle in a multidimensional dataset. On such data, which exhibits exploitable separations, diverse densities, etc., the quantum incremental k-means method performed well. The quantum platform enabled the development of a network of connected devices and electronic components by utilizing wireless hardware that was built from the ground up and a cutting-edge user interface. The incremental k-means algorithm and quantum platform, two emerging quantum technologies, will open previously unseen doors in science when combined.

**Author Contributions:** Conceptualization, S.D. and B.K.B.; methodology, S.D. and B.K.B.; software, S.D.; validation, S.D., B.K.B. and P.M.; formal analysis, S.D. and B.K.B.; investigation, S.D. and B.K.B.; resources, S.D.; data curation, S.D. and B.K.B.; writing—original draft preparation, S.D. and B.K.B.; writing—review and editing, S.D., B.K.B. and P.M.; visualization, S.D.; supervision, B.K.B. and P.M.; project administration, B.K.B. and P.M. All authors have read and agreed to the published version of the manuscript.

**Funding:** This research received no external funding.

**Institutional Review Board Statement:** Not applicable.

**Informed Consent Statement:** Not applicable.

**Data Availability Statement:** Data is unavailable due to privacy or ethical restrictions.

**Conflicts of Interest:** The authors declare no conflict of interest.

## References

1. Khalid, U.; urRehman, J.; Shin, H. Measurement-based quantum correlations for quantum information processing. *Sci. Rep.* **2020**, *10*, 2443. [[CrossRef](#)] [[PubMed](#)]
2. Kim, H.J.; Lee, S.; Lami, L.; Plenio, M.B. One-shot manipulation of entanglement for quantum channels. *IEEE Trans. Inf. Theory* **2021**, *67*, 5339–5351. [[CrossRef](#)]
3. Alloghani, M.; Al-Jumeily, D.; Mustafina, J.; Hussain, A.; Aljaaf, A.J. A systematic review on supervised and unsupervised machine-learning algorithms for data science. In *Supervised and Unsupervised Learning for Data Science*; Springer: Cham, Switzerland, 2020; pp. 3–21. [[CrossRef](#)]
4. De Amorim, R.C.; Mirkin, B. Minkowski metric, feature weighting and anomalous cluster initializing in K-Means clustering. *Pattern Recognit.* **2012**, *45*, 1061–1075. [[CrossRef](#)]
5. Kavitha, S.S.; Kaulgud, N. Quantum K-means clustering method for detecting heart disease using quantum circuit approach. *Soft Comput.* **2022**, 1–14. [[CrossRef](#)] [[PubMed](#)]
6. Devarajan, M.; Subramaniaswamy, V.; Vijayakumar, V.; Ravi, L. Fog-assisted personalized healthcare-support system for remote patients with diabetes. *J. Ambient. Intell. Humaniz. Comput.* **2019**, *10*, 3747–3760. [[CrossRef](#)]

7. Scheidsteger, T.; Haunschild, R.; Bornmann, L.; Ettl, C. Bibliometric analysis in the field of quantum technology. *Quantum Rep.* **2021**, *3*, 549–575. [[CrossRef](#)]
8. Rosch-Grace, D.; Straub, J. Analysis of the likelihood of quantum computing proliferation. *Technol. Soc.* **2022**, *68*, 101880. [[CrossRef](#)]
9. Bu, K. Quantum computing meets federated learning. *Sci. China Phys. Mech. Astron.* **2022**, *65*, 210331. [[CrossRef](#)]
10. Gitiaux, X.; Morris, I.; Emelianenko, M.; Tian, M. SWAP test for an arbitrary number of quantum states. *Quantum Inf. Process.* **2022**, *21*, 344. [[CrossRef](#)]
11. Giovannetti, V.; Lloyd, S.; Maccone, L. Quantum random access memory. *Phys. Rev. Lett.* **2008**, *100*, 160501. [[CrossRef](#)]
12. Crosson, E.J.; Lidar, D.A. Prospects for quantum enhancement with diabatic quantum annealing. *Nat. Rev. Phys.* **2021**, *3*, 466–489. [[CrossRef](#)]
13. Braine, L.; Egger, D.J.; Glick, J.; Woerner, S. Quantum algorithms for mixed binary optimization applied to transaction settlement. *IEEE Trans. Quantum Eng.* **2021**, *2*, 1–8. [[CrossRef](#)]
14. Kathuria, K.; Ratan, A.; McConnell, M.; Bekiranov, S. Implementation of a Hamming distance-like genomic quantum classifier using inner products on ibmqx2 and ibmq\_16\_melbourne. *Quantum Mach. Intell.* **2020**, *2*, 7. [[CrossRef](#)]
15. Biamonte, J.; Wittek, P.; Pancotti, N.; Rebentrost, P.; Wiebe, N.; Lloyd, S. Quantum machine learning. *Nature* **2017**, *549*, 195–202. [[CrossRef](#)]
16. Bai, L.; Song, Z.; Bao, H.; Jiang, J. K-means Clustering Based on Improved Quantum Particle Swarm Optimization Algorithm. In Proceedings of the 2021 13th International Conference on Advanced Computational Intelligence (ICACI), Wanzhou, China, 14–16 May 2021; pp. 140–145.
17. Boushaki, S.I.; Kamel, N.; Bendjeghaba, O. A new quantum chaotic cuckoo search algorithm for data clustering. *Expert Syst. Appl.* **2018**, *96*, 358–372. [[CrossRef](#)]
18. Javidi, B. 3D imaging with applications to displays, quantum imaging, optical security, and healthcare. In Proceedings of the 2015 14th Workshop on Information Optics (WIO), Kyoto, Japan, 1–5 June 2015; IEEE: Piscataway, NJ, USA, 2015; pp. 1–3. [[CrossRef](#)]
19. Singh, P.; Bose, S.S. A quantum-clustering optimization method for COVID-19 CT scan image segmentation. *Expert Syst. Appl.* **2021**, *185*, 115637. [[CrossRef](#)]
20. Kerenidis, I.; Landman, J. Quantum spectral clustering. *Phys. Rev. A* **2021**, *103*, 042415. [[CrossRef](#)]
21. Chen, J.; Qi, X.; Chen, L.; Chen, F.; Cheng, G. Quantum-inspired ant lion optimized hybrid k-means for cluster analysis and intrusion detection. *Knowl.-Based Syst.* **2020**, *203*, 106167. [[CrossRef](#)]
22. Qin, X.; Li, J.; Hu, W.; Yang, J. Machine Learning K-Means Clustering Algorithm for Interpolative Separable Density Fitting to Accelerate Hybrid Functional Calculations with Numerical Atomic Orbitals. *J. Phys. Chem. A* **2020**, *124*, 10066–10074. [[CrossRef](#)]
23. Bishwas, A.K.; Mani, A.; Palade, V. Quantum Algorithm for Sequence Clustering. In *Hybrid Intelligent Techniques for Pattern Analysis and Understanding*; CRC Press: Boca Raton, FL, USA, 2017; pp. 345–364.
24. Tang, E. Quantum principal component analysis only achieves an exponential speedup because of its state preparation assumptions. *Phys. Rev. Lett.* **2021**, *127*, 060503. [[CrossRef](#)]
25. Nivelkar, M.; Bhirud, S.G. Supervised Machine Learning Strategies for Investigation of Weird Pattern Formulation from Large Volume Data Using Quantum Computing. In *Advanced Computing and Intelligent Technologies*; Springer: Singapore, 2022; pp. 569–576. [[CrossRef](#)]
26. Thomas, C.; Charbonnier, J.; Garnier, A.; Bresson, N.; Bouchu, D.; Moreau, S.; Gustavo, F.; Vinet, M. Electrical and Morphological Characterizations of 3D Interconnections for Quantum Computation. *IEEE Trans. Compon. Packag. Manuf. Technol.* **2021**, *12*, 462–468. [[CrossRef](#)]
27. Aleksandrowicz, G.; Alexander, T.; Barkoutsos, P.; Bello, L. Qiskit: An Open-Source Quantum Computing Framework for Leveraging Today's Quantum Processors in Research, Education, and Business. Available online: <https://qiskit.org/> (accessed on 16 March 2019).
28. Acampora, G.; Schiattarella, R.; Vitiello, A. Using quantum amplitude amplification in genetic algorithms. *Expert Syst. Appl.* **2022**, *209*, 118203. [[CrossRef](#)]
29. Kwon, H.; Bae, J. Quantum amplitude-amplification operators. *Phys. Rev. A* **2021**, *104*, 062438. [[CrossRef](#)]
30. Lawless, W.F. Quantum-Like Interdependence Theory Advances Autonomous Human–Machine Teams (A-HMTs). *Entropy* **2020**, *22*, 1227. [[CrossRef](#)]
31. Poggiali, A.; Berti, A.; Bernasconi, A.; Del Corso, G.M.; Giudotti, R. Clustering Classical Data with Quantum k-Means. In Proceedings of the 23rd Italian Conference on Theoretical Computer Science, Roma, Italy, 7–9 September 2022.
32. Sinaga, K.P.; Yang, M.S. Unsupervised K-means clustering algorithm. *IEEE Access* **2020**, *8*, 80716–80727. [[CrossRef](#)]
33. Wu, J. Cluster analysis and K-means clustering: An introduction. In *Advances in K-Means Clustering*; Springer: Berlin/Heidelberg, Germany, 2012; pp. 1–16. [[CrossRef](#)]
34. Ohno, H. A quantum algorithm of K-means toward practical use. *Quantum Inf. Process.* **2022**, *21*, 146. [[CrossRef](#)]
35. Xu, L. Bayesian Ying–Yang machine, clustering and number of clusters. *Pattern Recognit. Lett.* **1997**, *18*, 1167–1178. [[CrossRef](#)]
36. Patil, P.; Karthikeyan, A. A survey on k-means clustering for analyzing variation in data. In *Inventive Communication and Computational Technologies*; Springer: Singapore, 2020; pp. 317–323. [[CrossRef](#)]

- 
37. Dataset Link. Available online: <https://www.kaggle.com/datasets/sulianova/cardiovascular-disease-dataset> (accessed on 27 September 2021).
  38. Hastie, T.; Tibshirani, R.; Friedman, J.H.; Friedman, J.H. *The Elements of Statistical Learning: Data Mining, Inference, and Prediction*; Springer: New York, NY, USA, 2009; Volume 2, pp. 1–758. [[CrossRef](#)]

**Disclaimer/Publisher’s Note:** The statements, opinions and data contained in all publications are solely those of the individual author(s) and contributor(s) and not of MDPI and/or the editor(s). MDPI and/or the editor(s) disclaim responsibility for any injury to people or property resulting from any ideas, methods, instructions or products referred to in the content.